An algebraic model to determine substrate kinetic parameters by global nonlinear fit of progress curves

Anal. Biochem. **2016** • DOI: 10.1016/j.ab.2016.11.001

Mey Ling Reytor González[a], Susan Cornell-Kennon[b], Erik Schaefer[b], Petr Kuzmič[*,a]

[a] *BioKin Ltd., Watertown, MA, USA*
[b] *AssayQuant Technologies Inc., Marlborough, MA, USA*

Abstract

We propose that the time course of an enzyme reaction following the Michaelis-Menten reaction mechanism can be conveniently described by a newly derived algebraic equation, which includes the Lambert Omega function. Following Northrop's ideas [*Anal. Biochem.* **321**, 457-461, 1983], the integrated rate equation contains the Michaelis constant (K_M) and the specificity number ($k_S \equiv k_{cat}/K_M$) as adjustable parameters, but not the turnover number k_{cat}. A modification of the usual global-fit approach involves a combinatorial treatment of nominal substrate concentrations being treated as fixed or alternately optimized model parameters. The newly proposed method is compared with the standard approach based on the "initial linear region" of the reaction progress curves, followed by nonlinear fit of initial rates to the hyperbolic Michaelis-Menten equation. A representative set of three chelation-enhanced fluorescence EGFR kinase substrates is used for experimental illustration. In one case, both data analysis methods (linear and nonlinear) produced identical results. However, in another test case, the standard method incorrectly reported a finite (50-70 μM) K_M value, whereas the more rigorous global nonlinear fit shows that the K_M is immeasurably high.

Key words: Enzyme kinetics; Nonlinear regression; Global fit; Lambert omega function; Integrated Michaelis-Menten equation

ARTICLE HISTORY:
Submitted 5 October 2016; Submitted in revised form 31 October 2016; Accepted 1 November 2016; Available online 4 November 2016

1. Introduction

Since the publication of Michaelis and Menten's seminal paper [1], numerous methods have emerged in analytical biochemistry for the determination of the Michaelis constant K_M, the turnover number k_{cat}, and the specificity number $k_S \equiv k_{cat}/K_M$, which taken together represent the most basic biochemical properties of enzyme substrates. For example, undergraduate level textbooks [2, p. 206] [3, p. 65] even to this day usually suggest determining the Michaelis constant from the linearized Lineweaver-Burk plot of transformed experimental data.

More specialized texts typically recommend determining the Michaelis constant by nonlinear fit of initial reaction rates to the Michaelis-Menten equation [4]. It is frequently assumed that the reaction progress curves contain an "initial linear region" [5], which presumably justifies the linear fit of data points contained in that region, as long as substrate conversion is kept below 10%. However, Cornish-Bowden [6, p. 87] has strongly challenged that assertion and claims instead that no more than 1% conversion is tolerable in order to define "true" initial rates. Cornish-Bowden's persuasive argument is that although many enzymatic reaction progress curves might *appear* linear, an imperceptible nonlinearity, which is literally invisible to the human eye, might strongly influence the ultimate results of the data analysis.

To address complications resulting from the nonlinearity problem, various authors have devised a range of data-analytic strategies. For example, Baici [7, pp. 55-56] recommends dividing the reaction progress curve into numerous short, approximately linear segments; computing the slope of each linear portion; and finally extrapolating the changing slopes to zero time.

Another distinctly different group of strategies is based on constructing a *nonlinear model for the entire reaction progress curve*; fitting this model to all the available data, not just to the presumed "initial linear" region; and finally extracting the substrate kinetic parameters from the results of the global fit without regard to the initial reaction rates. However, as an option, mathematical properties of each best-fit nonlinear model curve can be utilized to compute the first-derivative with respect to time, at time zero, as the initial reaction rate. The new data-analytic approach presented in this report falls into this latter category.

To arrive at the current method, we combined several ideas

*Corresponding author. BioKin Ltd., 15 Main St Ste 232, Watertown MA 02472, USA. Email address: pksci01@biokin.com

already existing in the biochemical literature. The foundation has been laid by Schnell and Mendoza's [8] discovery of a closed-form algebraic formula that can be used to represent the time course of an enzyme reaction conforming to the Michaelis-Menten mechanism. An important advantage of this algebraic solution is that it allows a significantly higher speed of computation, when compared either to the Newton-Raphson iterative scheme [9, 10] or to numerical integration of ODE systems [11].

Secondly, we took advantage of Northrop's realization [12] that 'V/K' (closely related to the specificity number k_{cat}/K_M) can, and probably should, be profitably treated as a *primary* biochemical parameter rather than a "derived" ratio. The advantage of Northrop's approach is that in many unfavorable cases, when neither K_M nor k_{cat} are well defined by the available data (see below for an illustrative example), the specificity number k_S is never-the-less very well defined.

Another element of the approach newly proposed here is the *global analysis* method advocated by Beechem [13]. Reported here is the first instance of a closed-form algebraic solution of the integrated Michaelis-Menten rate law, based on Lambert's Omega function, applied in the global analysis context. However, we propose an improvement over the usual approach in that some, but very importantly not all, nominal substrate concentrations are treated as adjustable model parameters rather than as fixed constants.

A comparison of our newly proposed nonlinear global fit method with the standard approach, based on the simplifying assumption of linearity in the reaction progress, is made possible by utilizing three chelation-enhanced fluorescence (CHEF) [14–17] substrates of the EGFR kinase. We show that in some cases the simplified standard method leads to results that are essentially identical to those offered by the rigorous nonlinear global fit. However, in other cases the simplified standard method completely fails, without any meaningful diagnostics, such as for example the correlation coefficients, R^2; the distribution of residuals; or confidence intervals for model parameters, that could be otherwise used by the data analyst to uncover the failure of the standard method.

2. Methods

2.1. Experimental

2.1.1. Materials

The EGFR protein kinase domain, amino acids 668-1210, was purchased from BPS Bioscience (Cat. No. 40187, Lot No. 120321-GC). Chelation-enhanced fluorescence substrates **Sub006**, **Sub009** and **Sub013**, containing the unnatural fluorogenic amino-acid Sox [14–17], were synthesized by standard solid-phase peptide synthesis methods and either purified by preparative reverse-phase HPLC (**Sub006**, **Sub013**) or desalted (**Sub009**), followed by rigorous analysis and quality control.

Sox-based substrates used in this study were experimental sequences selected to illustrate relevant data-analytic and mathematical procedures. Each of these substrates are now available from AssayQuant Technologies Inc. (Marlborough, Massachusetts). **Sub006** (Cat. No. AQT0008) sequence is Ac-EEEEYF-C(Sx)-LV-NH_2. **Sub009** (Cat. No. AQT0097) sequence is Ac-EEPEYI-C(Sx)-FG-NH_2. AQT0008 and AQT0097 are covered under US provisional patent application 62/331,903. **Sub013** (Cat. No. AQT0001) sequence is Ac-EEEEYI-C(Sx)-IV-NH_2, which has also been published as Omnia Y12, formerly available from Thermo Fisher Scientific.

2.1.2. Assay conditions

The EGFR kinase was assayed at the concentration of either 5 nM or 8 nM, depending on the substrate present at concentrations up to 50 μM, using a 1:2 dilution series. The assay buffer contained 50 mM HEPES pH 7.5, 1 mM ATP, 1 mM DTT, 0.01% Brij-35, 5% glycerol, 0.5 mM EGTA, 10 mM $MgCl_2$, and 250 μM $MnCl_2$. Fluorescence changes were monitored at 30°C for 90 or 120 minutes, depending on the substrate.

2.2. Theoretical

2.2.1. Model equation for data fitting

Here we propose that the time course of an enzyme reaction following the Michaelis-Menten kinetic mechanism [18, p. 19] can be conveniently described by a newly derived Eqns (1)–(2), where F_α is some appropriate experimental variable, such as for example fluorescence, recorded at the reaction time t; F_0 is the experimental signal observed at $t = 0$ (i.e., baseline offset – essentially a property of the instrument); $[S]_0$ is the initial substrate concentration; K_M is the Michaelis constant; and r_P is the specific molar response coefficient of the reaction product. The auxiliary variable α represents the value of the *Lambert omega* function, also referred to as Lambert W function [8, 19, 20]. In Eqn (2), $[E]_0$ is the concentration of the enzyme active sites; t is the reaction time; and k_S is the *specificity number* defined as k_{cat}/K_M. Note that k_S has the dimension of a second-order (bimolecular association) rate constant. We chose the particular symbol k_S to represent the specificity number on the basis of a recommendation from the International Union of Biochemistry [21, 22], which recommends the notation k_A, k_B for enzyme reactions involving substrates "A" and "B", respectively. Eqn (3) represents the *instantaneous observed reaction rate*, i.e., the first derivative with respect to time t of the physical variable F being monitored.

$$F_\alpha = F_0 + r_P\,([S]_0 - K_M\,\alpha) \tag{1}$$

$$\alpha = \omega\left[\frac{[S]_0}{K_M}\,\exp\left(\frac{[S]_0}{K_M} - k_S\,[E]_0\,t\right)\right] \tag{2}$$

$$\frac{dF_\alpha}{dt} = r_P\,k_S\,K_M\,[E]_0\,\frac{\alpha}{1+\alpha} \tag{3}$$

An alternate, algebraically equivalent, way of expressing the integrated rate law is given by Eqns (4)–(5). In this case the equation system does not contain K_M as a model parameter, but rather k_{cat} (and k_S). The alternate use of Eqn (1) or Eqn (4) depends on which of K_M or k_{cat} is of greater interest to the investigator.

$$F_\beta = F_0 + r_P \left([S]_0 - \frac{k_{cat}}{k_S} \beta \right) \quad (4)$$

$$\beta = \omega \left[[S]_0 \frac{k_S}{k_{cat}} \exp\left([S]_0 \frac{k_S}{k_{cat}} - k_S\ [E]_0\ t \right) \right] \quad (5)$$

The derivation of Eqns (1)–(2) is shown in Appendix A. The derivation of the instantaneous rate equation Eqn (3) is shown in Appendix B.

2.2.2. *Global data fitting procedure*

In the preliminary stages of developing our data-analytic method, we observed that in some particular cases the least-squares solution depended strongly on whether or not the nominal substrate concentrations were treated as fixed constants or, alternately, as adjustable model parameters. We also observed that it is not feasible to allow all substrate concentrations, without exception, to be treated as fitting parameters, because in that case the regression model becomes redundant with respect to several nonlinear parameters, such as for example the molar responses coefficient of the product.

To address this difficulty, we developed a heuristic multi-step data fitting procedure, as follows. We perform three separate rounds of global [13] nonlinear least squares fit. In each round, we treat *one* of the substrate concentration as a fixed parameter, while all remaining substrate concentrations are treated as adjustable parameters. More specifically, the three highest substrate concentrations are in turn treated as fixed constants. We subsequently compute the geometric mean and geometric standard deviation of the three separate sets of best-fit values of K_M and k_S.

All nonlinear regression analyses were performed by using the software package DynaFit [11] implementing the trust-region adaptive algorithm [23–25] (NL2SOL ver. 2.3).

2.2.3. *The "standard" method*

The conventional or standard method of determining substrate kinetic parameters consists of two separate steps. In step one, one must identify an "initial portion" of each reaction progress curve, and perform a *linear fit* of time vs. experimental signal values to determine the "initial rate" of the reaction. Here the fitting model is Eqn (6), where F is again the experimental signal observed at time t; F_0 is the baseline offset parameter; and v is the observed reaction rate in appropriate units (for example, relative fluorescence units per minute or per second). In step two, the initial rates are usually analyzed by a nonlinear fit to the Michaelis-Menten Eqn (7).

$$F = F_0 + v\,t \quad (6)$$

$$v = V_{max} \frac{[S]_0}{[S]_0 + K_M} \quad (7)$$

For the purpose of verifying our results, obtained with the newly derived mathematical model, we also deployed the conventional method, as described above, with one variation. In particular, in a trial-and-error fashion, we defined the "initial linear" region of each progress curve by taking into account a different number of data points, starting from $n_D = 4$ ($t_{max} = 9$ min) up to $n_D = 10$ ($t_{max} = 30$ min).

3. Results

3.1. *Example 1: Substrate* **Sub013**

The EGFR kinase was assayed with substrate **Sub013** at five different concentrations spanning from 3.125 μM to 50 μM, stepping by a factor of two. The resulting five reaction progress curves were combined into a single *global* [13] data set and subject to nonlinear regression analysis using Eqn (1) as the fitting model. The results are graphically shown in *Figure 1* and numerically in *Table 1*. The instantaneous observed rate plot is shown in *Figure 2*.

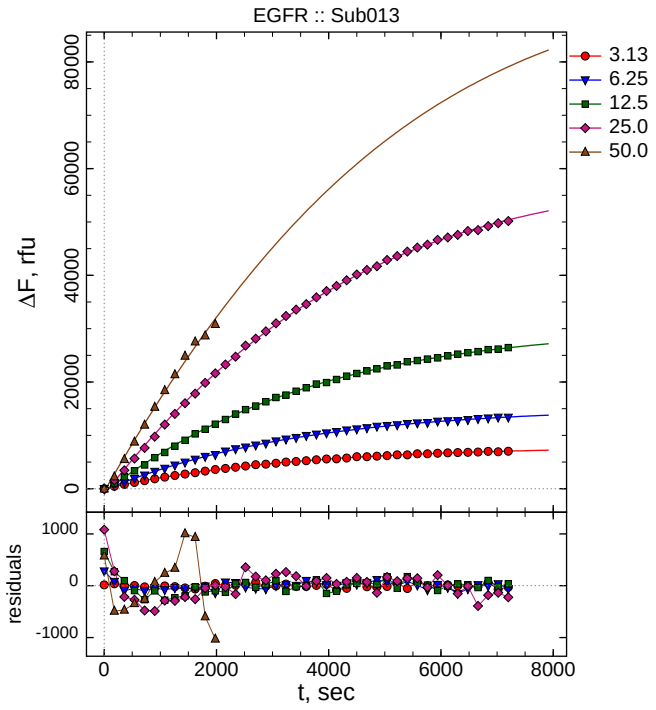

Figure 1: Global fit of kinetic data for substrate **Sub013**. Symbols represent fluorescence readings at the given reaction time. Smooth curves represent least-squares model curves generated by *global* fit of the combined kinetic traces to Eqn (1). Figure legend shows substrate concentrations in μM units. For more details see text.

In the particular instance illustrated in *Figure 1* and *Table 1*, the nominal substrate concentration $[S]_0^{(5)} = 50\ \mu$M was treated as a fixed model parameter, whereas the remaining four concentrations were treated as adjustable parameters. Note that the best-fit values of $[S]_0^{(1)}$ – $[S]_0^{(4)}$ are approximately 20% higher than the corresponding nominal concentrations.

Similar results were obtained when $[S]_0^{(4)} = 25\ \mu$M or $[S]_0^{(3)} = 12.5\ \mu$M were treated in turn as fixed parameters, while the four remaining substrate concentrations were optimized. In

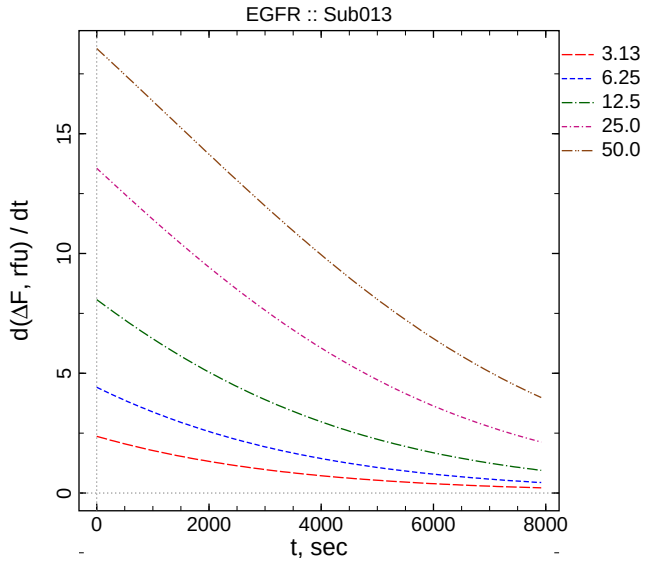

Figure 2: Instantaneous reaction rates corresponding to the best-fit theoretical model curves displayed in *Figure 1*. Each instantaneous rate curve was generated from Eqn (3), using the best-fit values of model parameters. Note that the reaction rate decreases rapidly *immediately from the start*.

each of the tree alternate regression analyses, we obtained three sets of slightly different best-fit values of K_m and r_P, while the specificity number k_S showed virtually no variation. The final results of this kinetic analysis were the geometric means and geometric standard deviations, $K_M = (67.0 \pm 7.4)\ \mu M$ and $k_S = 0.039\ \mu M^{-1}s^{-1}$. The geometric mean and geometric standard deviation of the turnover number computed as $k_S \times K_M$ was $k_{cat} = (2.6 \pm 0.3)\ s^{-1}$. Exactly identical results for k_{cat} were obtained when Eqns (4)–(5) were applied to the particular experimental data set. The mean and standard deviation of the difference response coefficient of the fluorescent product was $r_P = (2250 \pm 260)$ rfu/μM.

#	Parameter	Initial	Final ± Std.Err.	Cv,%
1	k_S, $\mu M^{-1}s^{-1}$	1	0.0393 ± 0.001	2.5
2	K_m, μM	100	78.3 ± 9.3	11.9
3	r_P, rfu/μM	1000	1933 ± 36	1.9
4	$[S]_0^{(1)}$, μM	3.13	4.10 ± 0.12	2.9
5	$[S]_0^{(2)}$, μM	6.25	8.00 ± 0.19	2.4
6	$[S]_0^{(3)}$, μM	12.50	15.99 ± 0.37	2.3
7	$[S]_0^{(4)}$, μM	25.00	31.17 ± 0.68	2.2
	$[S]_0^{(5)}$, μM	50.00	fixed	

Table 1: Results of global fit of kinetic data for substrate **Sub013**. The best-fit values of the five optimized offsets on the signal axis (F_0) are omitted for brevity. For further details see text.

3.2. *Example 2: Substrate* **Sub006**

The global fitting results for substrate **Sub006** were very similar to those shown in Section 3.1. This substrate is included principally because it enabled an important comparison between the results obtained by our newly proposed nonlinear global method and the standard method (see below).

3.3. *Example 3: Substrate* **Sub009**

The EGFR kinase was assayed with substrate **Sub009** at six different concentrations spanning from 0.78 μM to 25 μM, stepping by a factor of two. The resulting six reaction progress curves were combined into a single data set and subject to nonlinear regression analysis using Eqn (1) as the fitting model. The results are shown graphically in *Figure 3* and numerically in *Table 2*.

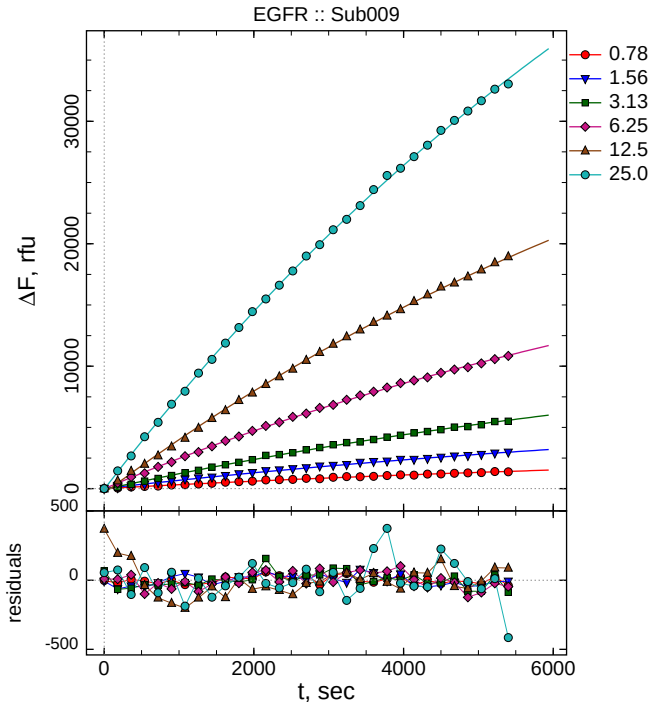

Figure 3: Global fit of kinetic data for substrate **Sub009**. Symbols represent fluorescence readings at the given reaction time. Smooth curves represent least-squares model curves generated by *global* fit of the combined kinetic traces to Eqn (1). Figure legend shows substrate concentrations in μM units. For more details see text.

Despite the fact that the data and model curves displayed in *Figure 3* (substrate **Sub009**) appear to show the same overall shape as the progress curves in *Figure 1* (substrate **Sub013**), the best-fit values of adjustable model parameters listed in *Table 2* illustrate a *fundamental* difference between the two substrates.

In particular, the Michaelis constant for **Sub009** cannot be determined because the best-fit value approached the upper limit imposed by the parameter constraints. We can safely conclude from this result that the true value of K_M must be much higher than the highest substrate concentration used in the experiment,

#	Parameter	Initial	Final ± Std.Err.	Cv,%
1	k_S, $\mu M^{-1}s^{-1}$	1	0.0196 ± 0.0012	6.1
2	K_m, μM	100	> 10000	> 10000
3	r_P, rfu/μM	1000	3260 ± 70	2.3
4	$[S]_0^{(1)}$, μM	0.78	1.05 ± 0.05	4.4
5	$[S]_0^{(2)}$, μM	1.56	2.21 ± 0.07	2.9
6	$[S]_0^{(3)}$, μM	3.13	4.22 ± 0.10	2.3
7	$[S]_0^{(4)}$, μM	6.25	8.13 ± 0.15	1.8
8	$[S]_0^{(5)}$, μM	12.5	14.35 ± 0.16	1.1
	$[S]_0^{(6)}$, μM	25.0	fixed	

Table 2: Results of global fit of kinetic data for substrate **Sub009**. The best-fit values of the six optimized offsets on the signal axis (F_0) are omitted for brevity. For further details see text.

in this case $[S]_0 = 25\ \mu M$. For the same reason, the upper limit for $k_{cat} = k_S \times K_M$ cannot be determined either. A systematic confidence interval search using the profile-t method [26] (details not shown) provided the lower limit estimates $K_M = 190\ \mu M$ and $k_{cat} = 4.3\ s^{-1}$. In this example, the application of Eqns (4)–(5) was unsuccessful in that it was not possible to determine k_{cat}, for the same reason that Eqns (1)–(2) did not produce a best-fit value of K_M. In fact, as a general rule, if K_M is undefined because the reaction progress curves are essentially exponential, the k_{cat} value is not defined either.

Most importantly, despite the fact that neither k_{cat} nor K_M can be defined by the available data, even at an approximate level, the *specificity number* $k_S \equiv k_{cat}/K_M$ *is well defined*, as is evidenced by the relatively low value (corresponding to 6% coefficient of variation) of the formal standard error $0.020 \pm 0.001\ \mu M^{-1}s^{-1}$.

Repeating this analysis while treating either $[S]_0^{(5)}$ or $[S]_0^{(4)}$ as fixed parameters produced essentially identical results as are those listed above in *Table 2*. The Michaelis constant and turnover numbers were undefined, whereas the best-fit value of the specificity number k_S was the same in all three cases.

3.4. Comparison with the standard method

The three EGFR kinase substrates discussed in this report were selected as illustrative examples in particular because they display substantially different behavior in the method comparison study discussed in this section. The main difference between the three substrates relies on how the K_M values determined by the standard method depend on the choice of t_{max}, i.e., the length of the "initial" portion of the reaction progress curves.

In one case (substrate **Sub013**), varying t_{max} between 9 and 30 minutes (stepping by 3 minutes to produce 8 distinct K_M values) had virtually no effect on the best-fit values of the Michaelis constant. For this particular substrate, all K_M determinations resulted in the best-fit values ranging from approximately 60 μM to 65 μM. The best-fit value of K_M for **Sub013**, as determined by our newly proposed global nonlinear method, was (67 ± 7) μM. Thus, in this case, not only the standard method results are entirely insensitive to the choice of t_{max} between 9 and 30 minutes, but also the results are essentially indistinguishable from those obtained by global nonlinear regression. These findings are illustrated by the blue filled circles in *Figure 4*. The empirical model curve passing through those data points is described by the empirical equation $K_M = -0.0494\, t_{max} + 64.1$.

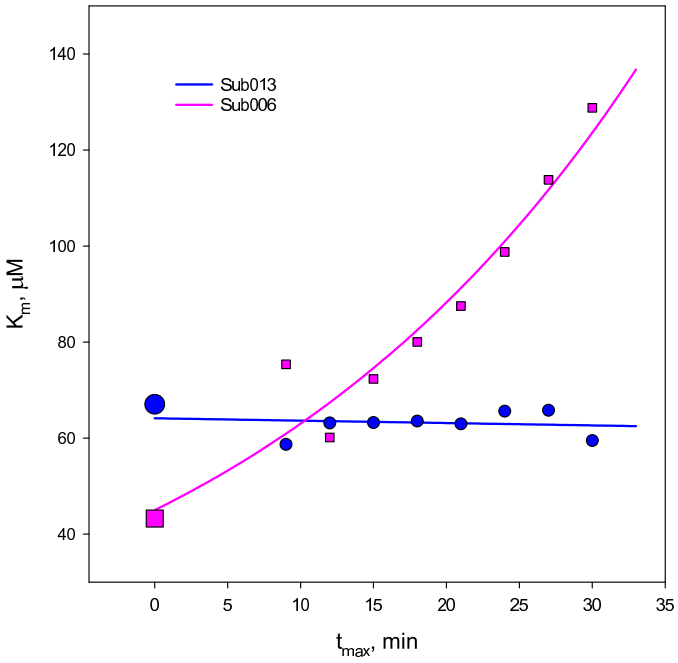

Figure 4: Comparison with the standard method for substrates **Sub006** and **Sub013**. The smaller size symbols (circles and squares) represent the results obtained by the standard method while varying the length of the "initial" portion between 9 and 30 minutes. The larger symbols located at $t_{max} = 0$ represent the best-fit values obtained by nonlinear regression.

In the second case (substrate **Sub006**), varying t_{max} from 9 to 30 minutes caused a prominent *increase* in the apparent K_M value determined by the standard method. This is shown as the smaller purple squares in *Figure 4*. Specifically, each additional time-point taken into the determination of initial rates (9, 12, 15, ... 30 min) ultimately increased the best-fit value of K_M by about 10 μM (from 60 μM to 140 μM). Importantly, when the varying values of K_M are extrapolated to (hypothetically) "zero duration" of the initial section, the extrapolated value is identical with the best-fit value determined by global nonlinear regression (large square in *Figure 4*). The nonlinear extrapolation curve shown in *Figure 4* is described by the exponential equation $K_M = 44.9 \exp(0.0337\, t_{max})$. The K_M measurement at $t_{max} = 9$ min for substrate **Sub006** appears to be an outlier from the exponential trend. The explanation lies in that this particular measurement, $K_M = 75\ \mu M$, was affected by large uncertainty as measured by the nonsymmetrical confidence interval determined by the profile-t method of Bates and Watts [26, 27]. In particular, the lower and upper limits at the 95% confidence level were 37 μM and 370 μM, respectively. Thus, within the rather large uncertainty the seemingly outlying K_M value does fit the overall pattern.

In the third and final scenario, varying t_{max} from 9 to 30 minutes caused a prominent *decrease* in the apparent K_M value determined by the standard method, as shown in *Figure 5*. Nominally, the values of K_M varied from approximately K_M = 200 μM at t_{max} = 9 min to approximately K_M = 70 μM at t_{max} = 30 min. The smooth curve in *Figure 5* is described empirically by the power function $K_M = 1210\, t_{max}^{-0.854}$.

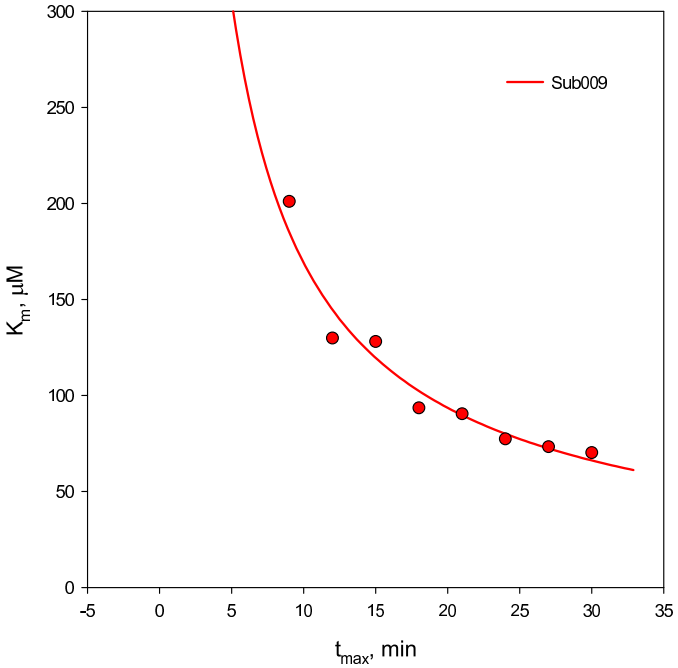

Figure 5: Comparison with the standard method for substrate **Sub009**. The circles represent the results obtained by the standard method while varying the length of the "initial" portion between 9 and 30 minutes. In this case, the best-fit value of K_M determined by global nonlinear regression tends to *infinity* and therefore no value for it is shown.

In the case of **Sub009**, the largest discrepancy between the results of the newly proposed nonlinear global method as compared with the classic standard method is observed for t_{max} = 30 min, i.e., when the first ten time points (amounting to 30 minutes) were considered as the "initial linear" region of the reaction progress curves. It is therefore valuable to examine the t_{max} = 30 min results in greater detail, to see if we could identify why the standard method produced K_M = (70 ± 14) μM, whereas the global nonlinear method leads to the conclusion that the K_M for **Sub009** is immeasurably high (thus, effectively "infinite").

The results of linear fit of individual reaction progress curves (only the first 10 time points in each case) are summarized graphically in *Figure 6*. The residual plots (bottom panel) show only a barely perceptible deviation from the linear model, and only for the progress curve obtained at $[S]_0$ = 25 μM. All residuals of fit span from approximately -100 to +100 relative fluorescence units (RFUs). At the same time, the overall amplitude of the experimental signal is 15×10^3 RFUs, which means that the random noise level is acceptably low, amounting to approximately 200/15000 = 1.3%.

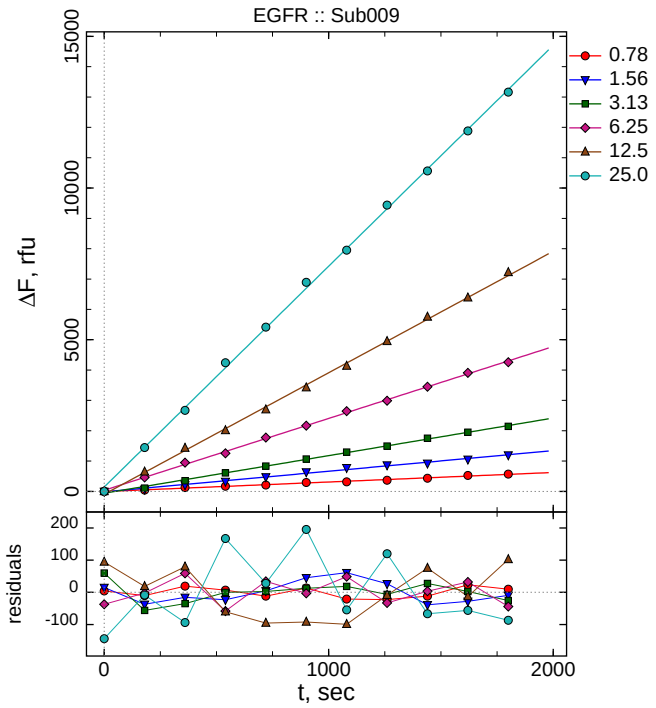

Figure 6: Linear fit of individual reaction progress curves for substrate **Sub009**. The figure legend shows substrate concentrations in μM units. The coefficient of determination, R^2, ranges from 0.993 at $[S]_0$ = 0.78 μM to 0.999 at $[S]_0$ = 25 μM. For additional details see text.

The correlation coefficients, R^2, for individual progress curves, starting at the lowest concentration $[S]_0$ = 0.78 μM and progressing toward $[S]_0$ = 25 μM, are 0.993, 0.993, 0.998, 0.999, 0.999, and 0.999. Thus, there is no indication of non-linearity based either on the visual examination of the residuals, or on the numerical value of the R^2. Based on either of these measures of potential nonlinearity, we are led to the conclusion that all progress curves displayed in *Figure 6* are "perfectly linear", within the first 30 minutes. However, we note that this conclusion is in conflict with those that can be drawn by a simple visual examination of the full reaction progress (t_{max} = 120 min), shown in *Figure 3*. The plots in *Figure 3* are clearly *nonlinear*, in their *entirety*, whereas the plots in *Figure 6* appear *linear*. However, the reaction progress curves cannot be linear and nonlinear at the same time. This important issue is addressed in greater detail in the Discussion.

The "initial" reaction rates corresponding to the linear fits shown in *Figure 6* are displayed in *Figure 7*. The best-fit values are listed in the figure legend. The non-symmetrical confidence interval for the Michaelis constant, obtained by the profile-*t* method of Bates & Watts [26, 27], spans from 44 μM to 140 μM at the 95% confidence level. Thus, there is no indication that the K_M would be undefined by the available experimental data, in which case the upper limit of the non-symmetrical confidence interval would tend to numerical infinity at 95% confi-

dence level.

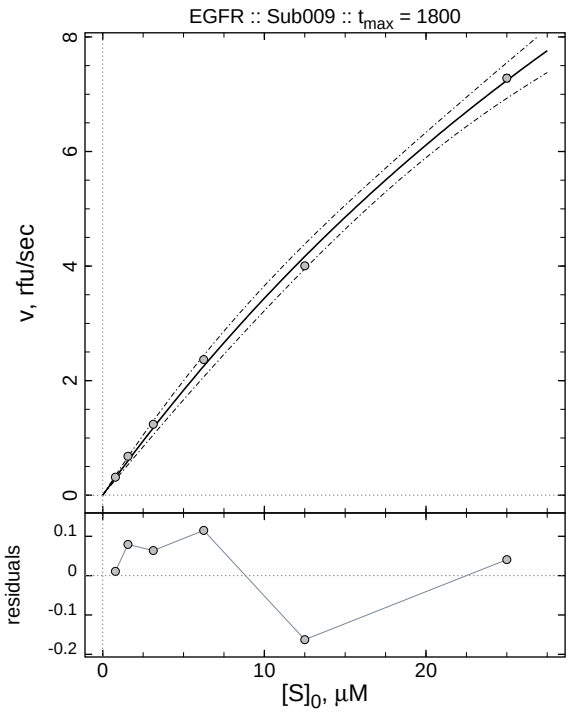

Figure 7: Nonlinear fit of "initial" reaction rates obtained from the linear fit of reaction progress curves shown in *Figure 6* to the Michaelis-Menten Eqn (7). The best-fit values of model parameters and associated formal standard errors are K_M = (70 ± 14) μM and V_{max} = (28 ± 4) rfu/sec.

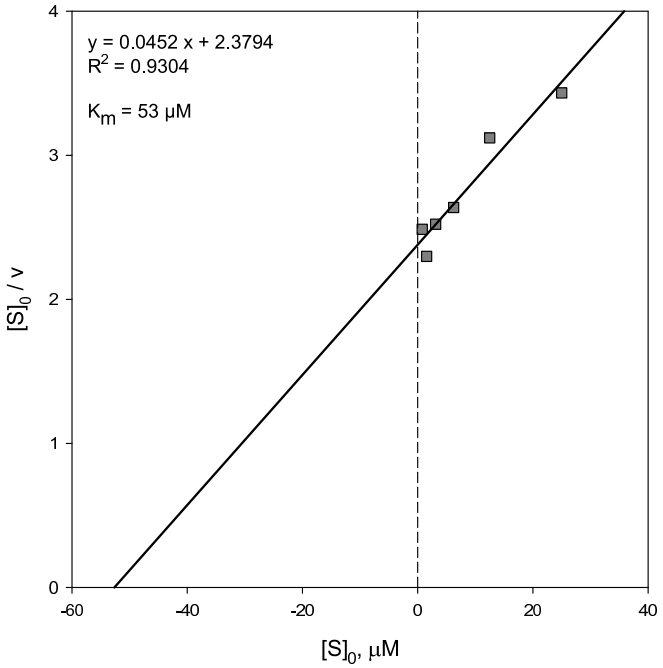

Figure 8: Hanes-Woolf replot of "initial" rate data for substrate **Sub009** displayed in *Figure 7*.

Not only is the 95% confidence interval for the K_M (as determined by the standard method) closed from both ends, but also the classic linearized re-plots of the "initial" reaction rates do not indicate any departure from the expected Michaelis-Menten kinetics. To verify this, we have constructed Lineweaver-Burk plots, Eadie-Hofstee plot, and Hanes-Woolf plots of the experimental data displayed in *Figure 7*. The Hanes-Woolf plot in particular is shown in *Figure 8*. The Michaelis constant computed from the slope and intercept of the replot is K_M = 53 μM. Recall that the newly proposed global nonlinear fit of the complete progress curves suggests that the K_M value is very much higher, to the extent that the upper limit of the 95% confidence level interval cannot be determined at all.

4. Discussion

In this paper we present for the first time a variant of a previously known closed-form algebraic model [8], which allows the fitting of enzymatic reaction progress curves to the integrated Michaelis-Menten rate law expressed by using the Lambert Omega function. The beneficial variation we introduce is based on Northrop's idea [12] that the specificity number $k_S \equiv k_{cat}/K_M$ should be considered as a "primary" kinetic parameter, rather than a "derived" kinetic constant. Also for the first time, we applied the integrated Michaelis-Menten rate law in the context of global fit [13]. Goličnik [20] previously utilized a similar kinetic model, also involving the Lambert Omega function, for global kinetic analysis of combined kinetics for simulating surface plasmon resonance experiments. However, this paper presents the first instance of performing a global fit using an integrated form of the Michaelis-Menten equation based on Lambert's Omega function.

The data-analytic method presented in this paper offers at least three major advantages. First, the method requires fewer data points and experiments, compared to the standard method. In fact, because there are only four adjustable model parameters per progress curve (K_M, k_S, F_0 and r_P), a small multiple of that particular number (typically at most 15-20 time-points) would be sufficient to determine all substrate kinetic parameters if the experimental data are of good quality. In favorable cases, it is necessary to only utilize a single substrate concentration, provided that the concentration is moderately higher that the K_M. For example, Goudar *et al.* [19] have analyzed a series of enzymatic progress curves recorded at different initial substrate concentrations, and obtained essentially identical K_M values in every case, based on the analysis of single individual curves.

The second major advantage is that this method provides more information about the biochemical system, from the same type of data that are normally used for initial rate studies. Specifically, if the reaction progress curves are at least partially developed (i.e., if substrate conversion reaches approximately 50%) it is possible to reliably estimate the molar response coefficient, for example, the UV/Vis extinction coefficient. This is because r_P appears directly as one of the regression parameters. Furthermore, assuming that the enzyme active site concentration $[E]_0$ can be trusted, and with the response coefficient in hand ("in-

ternal scaling" of the data from instrument coordinates to concentrations) we can directly estimate either the turnover number k_{cat} or the specificity number k_S.

Finally, the third major advantage is the relatively high speed of numerical processing, certainly in comparison with either certain ad-hoc algorithms based on the Newton-Raphson method [10], or in comparison with the numerical integration of ODE systems [11] arising in biochemical kinetics.

Regarding potential disadvantages and caveats, the present method is only applicable if and when the underlying kinetic mechanism strictly conforms to the simple Michaelis-Menten model. This means that Eqns (1)–(2), or alternately Eqns (4)–(5), are not applicable to continuous assays in which the enzyme undergoes partial denaturation, or in which the reaction product acts as an inhibitor. However, Goličnik [20] developed a variant of the mathematical model presented here, which allows not only for product inhibition, but also for full reversibility. On the other hand, in the context of possible departures from the simplest Michaelis-Menten kinetic model, Eqns (1)–(2) and Eqns (4)–(5) offer a possible approach to easily detecting such departures, because if a group of enzyme progress curves shows a clear lack of fit, as manifested in the distribution of residuals, then this provides positive evidence that the actual molecular mechanism is more complex.

Another drawback is that, at the present time, only relatively few commonly accessible software packages for data analysis offer an implementation of the Lambert Omega function. Those software packages include Mathematica, MATLAB, SAS, and most recently DynaFit [28].

In the process of comparing our results with those obtained by the standard method, which is based on linear fit of the "initial region" followed by the fit of the presumably "initial" reaction rates, we uncovered instances where the standard method failed without a discernible warning. For example, the standard method reported seemingly realistic values for substrate **Sub006** at every chosen length of the "initial" portion of the kinetic trace, and yet those results taken together showed a variation in the observed K_M values by several fold, which is unacceptable.

In the worst possible scenario, specifically in the case of substrate **Sub009**, we observed seemingly sensible results, as measured by multiple goodness-of-fit criteria. The coefficient of determination (R^2) values for the linear fit varied from 0.992 to 0.999 for all "initial" portions of the progress curves. The residual plots appeared nearly ideally random. The formal standard errors of K_M and V_{max} were relatively small. The nonsymmetrical confidence intervals were closed from both sides (upper and lower limit). The best-fit value of the Michaelis constant appeared realistic. The Hanes-Woolf replot of the linearly transformed data was linear and produced a realistic value of K_M.

And yet, the same time, the global nonlinear regression method revealed that the "best-fit" value of K_M produced by the standard method was invalid in the case of substrate **Sub009**. The reason for this failure has been eloquently explained by Cornish-Bowden [29, p. 40-41]. In particular, Cornish-Bowden pointed out that what may appear as a "linear" initial portion of the progress curve is in fact not strictly linear. This author recommended that only "if it is possible to arrange the assay so that less than 1% of the complete reaction is followed, it may be true that the progress curve is indistinguishable from a straight line." This is in contrast with frequently repeated rule of thumb referring to 10% (as opposed to merely 1%) conversion [30].

It is noteworthy that another instance of nonlinearity in CHEF reaction progress curves was previously reported to cause severe distortions of the overall results in the analysis of covalent inhibition [31]. In that particular case, similar to Example 3 reported here, the reaction progress curves *appeared* linear to the naked eye, but a rigorous mathematical analysis revealed that the relevant progress curves were actually nonlinear. As a consequence of ignoring the imperceptible nonlinearity, the inhibition constants were distorted by one order of magnitude [31].

In conclusion, the standard data analysis method based on linear fit of the "initial" portion reaction progress curves can be used reliably only if no variation in best-fit values of K_M and k_{cat} is seen in response to altering the t_{max} value. If, in fact, K_M and k_{cat} do depend on t_{max}, then the optimal choice for the data analyst is to utilize a nonlinear global analysis fit of complete progress curves, such as the one presented in this report, or alternately the Newton-Raphson iterative method of Duggleby [10].

At the present time, the relevant mathematical model (not only the Lambert Omega function but in fact Eqns (1)–(2)) is directly encoded in the software package DynaFit [28] (see Appendix C). A requisite technical note, input script files for the software, as well as illustrative data files, can be downloaded from the Technical Notes section of www.biokin.com.

The universality of the current method has been demonstrated by application to other systems beyond EGFR. Expanding this work is not practical for space reasons. However, step-by-step technical notes available online [32–34] demonstrate the use of the present method not only on EGFR [32], but also on proteases [33] and other enzymatic systems [34].

An anonymous reviewer requested that we present a "compelling justification" for the use of this new analysis method. The reviewer asked: "How bad is the initial velocity approach?" The answer to this question depends on the context. Let us consider that the K_M for substrate **Sub006** is distorted by a factor of two to four when determined by the initial velocity approach, as shown in *Figure 4*. In the *biological* context, a two-fold or even four-fold distortion of the true K_M value can probably be neglected. Many practicing biologists would agree that as long as substrate kinetic constants are correct within an order of magnitude, the estimates are "good enough" for understanding the enzyme's biological properties.

However, the situation changes dramatically in the *bioanalytical* context. For example, one of us (P.K.) served as consultant on a project involving the commercial release of a protease enzyme for therapeutic purposes [35–37]. In this case, a government regulatory agency demanded exquisitely high precision and accuracy in the determination of substrate kinetic constants before approving the injectable enzyme preparation for human use. A two-fold variation in the K_M would be con-

sidered unacceptable for the manufactured batch release assay. In any given context, both scientists and managers must consider an appropriate degree of formal rigor and choose the most appropriate biochemical analysis method.

The raw experimental data utilized in this report as well as all DynaFit [11, 28] input script files are available for download as a supplementary material [32]. The DynaFit software package is available free of charge to all academic researchers from http://www.biokin.com.

Acknowledgments

The authors thank Prof. Barbara Imperiali, Massachusetts Institute of Technology, Department of Biology, for helpful comments and suggestions to improve the manuscript.

Disclosure of Commercial Interest

AssayQuant Technologies Inc. (Marlborough, Massachusetts; www.assayquant.com) is a purveyor of commercially available synthetic peptides for protein kinase assays (Sox Technology Sensors) marketed under the trade mark PhosphoSense™. BioKin Ltd. (Watertown, Massachusetts; www.biokin.com) develops and distributes the DynaFit software package, available free of charge to all academic users and for a fee to for-profit organizations.

References

[1] L. Michaelis, M. Menten, Die kinetik der invertinwirkung, Biochem. Z. 49 (1913) 333–369.

[2] D. L. Nelson, M. M. Cox, Lehninger Principles of Biochemistry, 4th Edition, W. H. Freeman, San Francisco, 2004.

[3] R. K. Murray, D. K. Granner, P. A. Mayes, V. W. Rodwell, Harper's Illustrated Biochemistry, 26th Edition, Lange Medical Books/McGraw-Hill, New York, 2003.

[4] R. A. Copeland, Evaluation of Enzyme Inhibitors in Drug Discovery, 2nd Edition, John Wiley, New York, 2013.

[5] R. L. Stein, Kinetic of Enzyme Action: Essential Principles for Drug Hunters, J. Wiley and Sons, Inc., New York, 2011.

[6] A. Cornish-Bowden, Fundamentals of Enzyme Kinetics, 4th Edition, Wiley-VCH, Berlin, 2012.

[7] A. Baici, Kinetics of Enzyme-Modifier Interactions, Springer Verlag, Wien, 2015.

[8] S. Schnell, C. Mendoza, Closed form solution for time-dependent enzyme kinetics, J. theor. Biol. 187 (1997) 207–212.

[9] R. G. Duggleby, Estimation of the initial velocity of enzyme-catalysed reactions by non-linear regression analysis of progress curves, Biochem. J. 228 (1985) 55–60.

[10] R. G. Duggleby, Progress-curve analysis in enzyme kinetics: Numerical solution of integrated rate equations, Biochem. J. 235 (1986) 613–615.

[11] P. Kuzmič, Program DYNAFIT for the analysis of enzyme kinetic data: Application to HIV proteinase, Anal. Biochem. 237 (1996) 260–273.

[12] D. Northrop, Fitting enzyme-kinetic data to v/k, Anal. Biochem. 321 (1983) 457–461.

[13] J. M. Beechem, Global analysis of biochemical and biophysical data, Meth. Enzymol. 210 (1992) 37–54.

[14] M. D. Shults, D. Carrico-Moniz, B. Imperiali, Optimal Sox-based fluorescent chemosensor design for serine/threonine protein kinases, Anal. Biochem. 352 (2006) 198–207.

[15] E. Luković, J. A. González-Vera, B. Imperiali, Recognition-domain focused chemosensors: versatile and efficient reporters of protein kinase activity, J. Am. Chem. Soc. 130 (2008) 12821–12827.

[16] E. Luković, E. Vogel Taylor, B. Imperiali, Monitoring protein kinases in cellular media with highly selective chimeric reporters, Angew. Chem. Int. Ed. 121 (2009) 6960–6963.

[17] J. A. González-Vera, E. Luković, B. Imperiali, A rapid method for generation of selective Sox-based chemosensors of Ser/Thr kinases using combinatorial peptide libraries, Bioorg. Med. Chem. Lett. 19 (2009) 1258–1260.

[18] I. H. Segel, Enzyme Kinetics, Wiley, New York, 1975.

[19] C. T. Goudar, J. R. Sonnad, R. G. Duggleby, Parameter estimation using a direct solution of the integrated Michaelis-Menten equation, Biochim. Biophys. Acta 1429 (1999) 377–383.

[20] M. Goličnik, On the Lambert W function and its utility in biochemical kinetics, Biochem. Eng. J. 63 (2012) 116–123.

[21] A. Cornish-Bowden, Current IUBMB recommendations on enzyme nomenclature and kinetics, Perspectives in Science 1 (2014) 74–87.

[22] Nomenclature Committee of the International Union of Biochemistry, Symbolism and terminology in enzyme kinetics, Biochem. J. 213 (1983) 561–571.

[23] J. E. Dennis, D. M. Gay, R. E. Welsch, Algorithm 573: NL2SOL, ACM Trans. Math. Software 7 (1981) 369–383.

[24] J. E. Dennis, D. M. Gay, R. E. Welsch, An adaptive nonlinear least-squares algorithm, ACM Trans. Math. Software (1981) 348–368.

[25] J. E. Dennis, R. B. Schnabel, Numerical Methods for Unconstrained Optimization and Nonlinear Equations, Prentice-Hall, Upper Saddle River, NJ, 1983.

[26] D. G. Watts, Parameter estimation from nonlinear models, Methods Enzymol. 240 (1994) 24–36.

[27] D. M. Bates, D. G. Watts, Nonlinear Regression Analysis and its Applications, Wiley, New York, 1988.

[28] P. Kuzmič, DynaFit - A software package for enzymology, Meth. Enzymol. 467 (2009) 247–280.

[29] A. Cornish-Bowden, Fundamentals of Enzyme Kinetics, Butterworths, London, 1979.

[30] G. S. Sittampalam, N. P. Coussens, H. Nelson, M. Arkin, D. Auld, C. Austin, B. Bejcek, M. Glicksman, J. Inglese, P. W. Iversen, Z. Li, J. McGee, O. McManus, L. Minor, A. Napper, J. M. Peltier, T. Riss, O. J. Trask, J. Weidner, Assay Guidance Manual, https://www.ncbi.nlm.nih.gov/books/NBK92007/, [Online] (2004-).

[31] P. Kuzmič, J. Solowiej, B. W. Murray, An algebraic model for the kinetics of covalent enzyme inhibition at low substrate concentrations, Anal. Biochem. 484 (2015) 82–90.

[32] P. Kuzmič, Integrated Michaelis-Menten equation in DynaFit. 1. Application to EGFR protein kinase, BioKin Ltd Technical Note TN-2016-01, http://www.biokin.com/TN/2016/01, [Online] (2016-).

[33] P. Kuzmič, Integrated Michaelis-Menten equation in DynaFit. 2. Application to 5α-ketosteroid reductase, BioKin Ltd Technical Note TN-2016-02, http://www.biokin.com/TN/2016/02, [Online] (2016-).

[34] P. Kuzmič, Integrated Michaelis-Menten equation in DynaFit. 3. Application to HIV protease, BioKin Ltd Technical Note TN-2016-03, http://www.biokin.com/TN/2016/03, [Online] (2016-).

[35] A. Dwivedi, P. Roy-Chaudhury, E. Peden, B. Browne, E. Ladenheim, V. Scavo, P. Gustafson, M. Wong, M. Magill, F. Lindow, A. Blair, M. Jaff, F. Franano, S. Burke, Application of human type I pancreatic elastase (PRT-201) to the venous anastomosis of arteriovenous grafts in patients with chronic kidney disease, J. Vasc. Access 15 (2014) 376–384.

[36] J. Hye, R., E. Peden, T. O'Connor, B. Browne, B. Dixon, A. Schanzer, S. Jensik, L. Dember, M. Jaff, S. Burke, Human type I pancreatic elastase treatment of arteriovenous fistulas in patients with chronic kidney disease, J. Vasc. Surg. 60 (2014) 454–461.

[37] S. Burke, K. Macdonald, E. Moss, D. Bunton, B. Starcher, M. Wong, K. Bland, F. Franano, Effects of recombinant human type I pancreatic elastase on human atherosclerotic arteries, J. Cardiovasc. Pharmacol. 64 (2014) 530–535.

Appendix

A. Derivation of Eqn (1)

The instantaneous rate (i.e., reaction rate at the arbitrary time t) of an enzyme reaction following the Michaelis-Menten kinetic mechanism is given by Eqn (8), where [S] is the concentration of substrate at an arbitrary time t. This differential equation can be integrated analytically by the method of separation of variables, which yields Eqn (9), where $[S]_0$ is substrate concentration at the initial time $t = 0$. Note that it is algebraically impossible to further rearrange Eqn (9) so as to extract [S] on the left-hand side unless we resort to the Lambert ω function, as described below.

$$\frac{d[S]}{dt} = -k_{cat}\,[E]_0\,\frac{[S]}{[S]+K_M} \tag{8}$$

$$0 = [S] - [S]_0 + K_M \ln\frac{[S]}{[S]_0} + k_{cat}\,[E]_0\,t \tag{9}$$

In its general form, the Lambert ω function is the inverse of the function $f(x) = x\,e^x$, in the sense that $x = \omega\,(x\,e^x)$. Thus, even though it is possible to rearrange Eqn (9) so as to isolate [S] on the left-hand side, perhaps it is possible to rearrange Eqn (9) so as to extract [S] exp([S]). Indeed, if we can somehow corral [S] exp([S]) on the left-hand side of a rearranged Eqn (9), we could then "take the ω" of both sides. In so doing, we could directly obtain algebraic formula for the substrate concentration at time t, because by definition $[S] = \omega\left([S]\,e^{[S]}\right)$. This task is accomplished in a series of algebraic manipulations delineated below.

$$\ln\frac{[S]}{[S]_0} = \frac{[S]_0 - [S] - k_{cat}\,[E]_0\,t}{K_M}$$

$$[S] = [S]_0\,\exp\left(\frac{[S]_0 - [S] - k_{cat}\,[E]_0\,t}{K_M}\right)$$

$$[S]\,\exp\left(\frac{[S]}{K_M}\right) = [S]_0\,\exp\left(\frac{[S]_0 - k_{cat}\,[E]_0\,t}{K_M}\right)$$

$$\omega\left[\frac{[S]}{K_M}\,\exp\left(\frac{[S]}{K_M}\right)\right] = \frac{[S]}{K_M} = \omega\left[\frac{[S]_0}{K_M}\,\exp\left(\frac{[S]_0 - k_{cat}\,[E]_0\,t}{K_M}\right)\right]$$

$$[S] = K_M\,\omega\left[\frac{[S]_0}{K_M}\,\exp\left(\frac{[S]_0 - k_{cat}\,[E]_0\,t}{K_M}\right)\right]$$

For an enzyme reaction following the overall scheme $S \rightarrow P$, the product concentration at time t is by definition equal to $[P] = [S]_0 - [S]$. Thus, we obtain Eqn (10), in which $k_{cat}/K_M \equiv k_S$ is the specificity number.

$$[P] = [S]_0 - K_M\,\omega\left[\frac{[S]_0}{K_M}\,\exp\left(\frac{[S]_0}{K_M} - \frac{k_{cat}}{K_M}\,[E]_0\,t\right)\right] \tag{10}$$

Finally, the experimental signal F is related to the product concentration [P] as $F = F_0 + r_P[P]$, which leads directly to Eqn (1).

B. Derivation of Eqn (3)

The derivative of [S] with respect to time is given by

$$\begin{aligned}
\frac{\mathrm{d}[\mathrm{S}]}{\mathrm{d}t} &= \frac{\mathrm{d}}{\mathrm{d}t}\left\{K_\mathrm{M}\,\omega\left[\frac{[\mathrm{S}]_0}{K_\mathrm{M}}\,\exp\left(\frac{[\mathrm{S}]_0 - k_\mathrm{cat}\,[\mathrm{E}]_0\,t}{K_\mathrm{M}}\right)\right]\right\} \\
&= K_\mathrm{M}\,\frac{\mathrm{d}}{\mathrm{d}t}\left\{\omega\left[\frac{[\mathrm{S}]_0}{K_\mathrm{M}}\,\exp\left(\frac{[\mathrm{S}]_0 - k_\mathrm{cat}\,[\mathrm{E}]_0\,t}{K_\mathrm{M}}\right)\right]\right\} \\
&= K_\mathrm{M}\,\frac{\mathrm{d}}{\mathrm{d}t}\left\{\omega\left[g(t)\right]\right\} \\
g(t) &\equiv \frac{[\mathrm{S}]_0}{K_\mathrm{M}}\,\exp\left(\frac{[\mathrm{S}]_0 - k_\mathrm{cat}\,[\mathrm{E}]_0\,t}{K_\mathrm{M}}\right)
\end{aligned}$$

According to the chain rule of differential calculus,

$$\frac{\mathrm{d}\omega\left(g(t)\right)}{\mathrm{d}t} = \frac{\mathrm{d}\omega}{\mathrm{d}g}\cdot\frac{\mathrm{d}g}{\mathrm{d}t}$$

Thus,

$$\begin{aligned}
\frac{\mathrm{d}g}{\mathrm{d}t} &= -[\mathrm{E}]_0\,\frac{k_\mathrm{cat}}{K_\mathrm{M}}\,\frac{[\mathrm{S}]_0}{K_\mathrm{M}}\,\exp\left(\frac{[\mathrm{S}]_0 - k_\mathrm{cat}\,[\mathrm{E}]_0\,t}{K_\mathrm{M}}\right) \\
&= -[\mathrm{E}]_0\,\frac{k_\mathrm{cat}}{K_\mathrm{M}}\,g(t)
\end{aligned}$$

The rule for differentiating the Lambert Omega was presented by Golicnik [20, Eqn. (A3), p. 122]:

$$\frac{\mathrm{d}\omega(g(t))}{\mathrm{d}g(t)} = \frac{1}{g(t)}\,\frac{\omega(g(t))}{1+\omega(g(t))}$$

When the differentiation rule is applied in the present case, we obtain:

$$\begin{aligned}
\frac{\mathrm{d}\omega\left(g(t)\right)}{\mathrm{d}t} &= \frac{\mathrm{d}\omega}{\mathrm{d}g}\cdot\frac{\mathrm{d}g}{\mathrm{d}t} \\
&= -\frac{1}{g}\,\frac{\omega}{1+\omega}\cdot[\mathrm{E}]_0\,\frac{k_\mathrm{cat}}{K_\mathrm{M}}\,g \\
&= -\frac{k_\mathrm{cat}}{K_\mathrm{M}}\,[\mathrm{E}]_0\cdot\frac{\omega}{1+\omega} \\
\frac{\mathrm{d}[\mathrm{S}]}{\mathrm{d}t} &= -k_\mathrm{cat}\,[\mathrm{E}]_0\cdot\frac{\omega}{1+\omega}
\end{aligned}$$

The derivative of the experimental signal is given by $F = r_\mathrm{P}[\mathrm{P}] = r_\mathrm{P}([\mathrm{S}]_0 - [\mathrm{S}])$. Therefore $\mathrm{d}F/\mathrm{d}t = -r_\mathrm{P}\mathrm{d}[\mathrm{S}]/\mathrm{d}t$ and, finally,

$$\begin{aligned}
\frac{\mathrm{d}F}{\mathrm{d}t} &= r_\mathrm{P}\,k_\mathrm{cat}\,[\mathrm{E}]_0\,\frac{\omega}{1+\omega} \\
&= r_\mathrm{P}\,k_\mathrm{cat}\,[\mathrm{E}]_0\,\frac{\alpha}{1+\alpha} \qquad .
\end{aligned}$$

C. DynaFit input script

The DynaFit [28] script listed below was used to perform global nonlinear fit of combined progress curve data for substrate **Sub006**. Note that the maximum substrate concentration $[\mathrm{S}]_0 = 25\ \mu\mathrm{M}$ was held fixed at its nominal value, whereas the remaining substrate concentrations were treated as optimized parameters. This is indicated by the presence of the question mark following the given concentration value, for example `So = 3.13 ?`. The BioKin Technical Note No. 2016/01 contains electronic copies of all input data files (DynaFit scripts and raw experimental data) that were used to produce this report. Those materials are available for download from www.biokin.com/TN/2016/01/.

```
[task]
   task = fit
   data = generic
   code = built-in
[equation]
   MichaelisMentenProgressKmKs
[parameters]
   Eo = 0.008
   rP = 1000 ?
   kS = 1 ?
   Km = 100 ?
[data]
   variable t
   directory ./proj/CHEF/EGFR/progress/data
graph EGFR :: Sub006
   sheet DFit--EGFR--Sub006.csv
   column 2
      param Fo = 0 ? (-10000 .. 10000)
      param So = 3.13 ? | label 3.13
   column 3
      param Fo = 0 ? (-10000 .. 10000)
      param So = 6.25 ? | label 6.25
   column 4
      param Fo = 0 ? (-10000 .. 10000)
      param So = 12.5 ? | label 12.5
   column 5
      param Fo = 0 ? (-10000 .. 10000)
      param So = 25.0   | label 25.0
[output]
   directory ./proj/CHEF/EGFR/progress/output
[settings]
{Filter}
   ZeroBaselineSignal = y
{Output}
   XAxisLabel = t, sec
   YAxisLabel = {/Symbol D}F, rfu
   WriteTeX = y
[end]
```